AD A218 710

UNCLASSIFIED — MASTER COPY — FOR REPRODUCTION PURPOSES

SECURITY CLASSIFICATION OF THIS PAGE

# REPORT DOCUMENTATION PAGE

| | |
|---|---|
| 1a. REPORT SECURITY CLASSIFICATION: Unclassified | 1b. RESTRICTIVE MARKINGS |
| 2a. SECURITY CLASSIFICATION AUTHORITY | 3. DISTRIBUTION/AVAILABILITY OF REPORT: Approved for public release; distribution unlimited. |
| 2b. DECLASSIFICATION / DOWNGRADING SCHEDULE | |
| 4. PERFORMING ORGANIZATION REPORT NUMBER(S) | 5. MONITORING ORGANIZATION REPORT NUMBER(S) |
| 6a. NAME OF PERFORMING ORGANIZATION: Center of Excellence in AI, University of Pennsylvania; 6b. OFFICE SYMBOL (If applicable) | 7a. NAME OF MONITORING ORGANIZATION: U. S. Army Research Office |
| 6c. ADDRESS (City, State, and ZIP Code): Dept. of Computer & Information Science, 200 S. 33rd Street, Philadelphia, PA 19104-6389 | 7b. ADDRESS (City, State, and ZIP Code): P. O. Box 12211, Research Triangle Park, NC 27709-2211 |
| 8a. NAME OF FUNDING/SPONSORING ORGANIZATION: U. S. Army Research Office; 8b. OFFICE SYMBOL (If applicable) | 9. PROCUREMENT INSTRUMENT IDENTIFICATION NUMBER |
| 8c. ADDRESS (City, State, and ZIP Code): P. O. Box 12211, Research Triangle Park, NC 27709-2211 | 10. SOURCE OF FUNDING NUMBERS: PROGRAM ELEMENT NO. / PROJECT NO. / TASK NO. / WORK UNIT ACCESSION NO |

11. TITLE (Include Security Classification)
Image Segmentation with Detection of Highlights and Inter-Reflections Using Color (MS-CIS-89-39)

12. PERSONAL AUTHOR(S)
Ruzena Bajcsy, Sang Wook Lee, and Ales Leonardis

| 13a. TYPE OF REPORT | 13b. TIME COVERED | 14. DATE OF REPORT (Year, Month, Day) | 15. PAGE COUNT |
|---|---|---|---|
| Interim technical | FROM ____ TO ____ | June 1989 | 23 |

16. SUPPLEMENTARY NOTATION
The view, opinions and/or findings contained in this report are those of the author(s) and should not be construed as an official Department of the Army position, policy, or decision, unless so designated by other documentation.

| 17. COSATI CODES | | |
|---|---|---|
| FIELD | GROUP | SUB-GROUP |
| | | |
| | | |

18. SUBJECT TERMS (Continue on reverse if necessary and identify by block number)
Image processing, color

19. ABSTRACT (Continue on reverse if necessary and identify by block number)


We present an approach to the construction of a computational model for color image segmentation based on the physical properties of sensors, illumination lights and surface reflectances. Using the established model, we perform color image segmentation and detect small inter-reflections as well as highlights.


| | |
|---|---|
| 20. DISTRIBUTION/AVAILABILITY OF ABSTRACT: ☐ UNCLASSIFIED/UNLIMITED ☐ SAME AS RPT. ☐ DTIC USERS | 21. ABSTRACT SECURITY CLASSIFICATION: Unclassified |
| 22a. NAME OF RESPONSIBLE INDIVIDUAL | 22b. TELEPHONE (Include Area Code) / 22c. OFFICE SYMBOL |

DD FORM 1473, 84 MAR — 83 APR edition may be used until exhausted. All other editions are obsolete.

SECURITY CLASSIFICATION OF THIS PAGE
UNCLASSIFIED

# IMAGE SEGMENTATION WITH DETECTION OF HIGHLIGHTS AND INTER-REFLECTIONS USING COLOR

*Ruzena Bajcsy, Sang Wook Lee*
*and Aleš Leonardis*

MS-CIS-89-39
GRASP LAB 182

Department of Computer and Information Science
School of Engineering and Applied Science
University of Pennsylvania
Philadelphia, PA 19104

June 1989

**Acknowledgements:** This work was supported by the DuPont Corporation and by the following grants: Air Force AFOSR F49620-85-K-0018, ARPA N00014-88-K-0630, DARPA grant NOOO14-85-K-0018, NSF grants MCS-8219196-CER, IRI84-10413-AO2 and U.S. Army grants DAA29-84-K-0061, DAA29-84-9-0027.

Image Segmentation with Detection of Highlights and Inter-reflections Using Color

Ruzena Bajcsy, Sang Wook Lee and Aleš Leonardis*

Department of Computer and Information Science, University of Pennsylvania, Philadelphia, PA 19104

**Abstract**

We present an approach to the construction of a computational model for color image segmentation based on the physical properties of sensors, illumination lights and surface reflectances. Using the established model, we perform color image segmentation and detect small inter-reflections as well as highlights.

# 1 Introduction

Color is one of the major features in identifying objects, and color vision has been the most intensively studied sensory process in human vision. In machine vision, however, the use of color has not been the subject of active research, although color has recently received attention as a useful property for image segmentation and object recognition. The purpose of color vision is to extract aspects of the spectral property of object surfaces, while at the same time discounting various illuminations in order to provide useful information in image analysis. The most notable applications include recognition and identification of colored objects and image segmentation.

There have been approaches to image segmentation based on histograms of red (R), green (G) and blue (B) values or on transformed values such as YIQ [10] [11], or by using color edges in addition to intensity edges [9]. These algorithms are primarily extentions of intensity segmentation to

*Also at Fakulteta za elektrotehniko v Ljubljani, University of Ljubljana, Yugoslavia.

multidimensional processing with extra information provided by color. Thus they cannot distinguish between different edge types due to material changes, highlights, shading, and shadow.

Also, there has been an approach to detection of highlights by combining the traditional segmentation with physics-based post-processing [4]. Since traditional color image segmentation algorithms generally have not accounted for the influence of optical effects on object colors, the method suffers from many erroneous regions. If the physical models were included at the segmentation stage, many of these regions could be properly classified. The first physical approaches to color image understanding have been introduced only recently [1] [2]. Detection of highlights is acheived by clustering color points in RGB space using the dichromatic property of dielectric materials. Since the spectral curves of the camera and filters are not included in these models, the metric in the RGB space varies with the choice of the sensors.

In addition to highlights, shading and shadow, there are other impediments to observing real material changes such as variation of illumination and multiple reflections between objects. Objects receive not only the lights directly from illumination sources but also the reflected lights from other objects. The latter induces a change of the perceived surface color which we call inter-reflection. The process of discounting illuminations from the surface reflectance, namely color constancy, is a heavily studied subject in color vision [8] [6] [5], though successful applications are yet limited.

In this paper we present an approach to the construction of a computational model for color segmentation, not only with detection of highlights but with detection of small color changes induced by inter-reflections as well. We use the dichromatic model [1] for dielectric materials and develop a metric space based on the physical properties of sensors in order to better manipulate light-surface interactions.

We begin in Section 2 with sensing and metric representation of color in a machine vision system. In the following section, we describe a method of color constancy using a reference plate. In Section 4 a surface reflectance model is established from various mechanisms of surface reflections. Various

optical phenomena such as shading, shadow, highlights and inter-reflections between objects are explained in Section 5, in terms of the established surface reflectance model. In Section 6, we propose a method of segmentation and highlights and inter-reflection detection between objects. We present some of our initial results in Section 7, and suggestions for further studies are given in the following section.

## 2 Representation and Sensing of Color

Representation of color with finite-dimensional linear models has been a topic of many studies [12] [13] [7] [14]. There have been some approaches to obtaining characteristic basis functions by investigating many samples of daylight and surface reflectances [13] [12]. It has been suggested that although the number of basis functions required to completely describe full spectra is essentially infinite, a small number of basis functions can provide good spectral approximations of most natural illuminants and surface reflectances. Our approach is to represent measured colors in a metric space in order to better manipulate physical properties of surface colors for image segmentation.

Both for surface reflectance and for illumination, we here use the first three Fourier bases for their mathematical simplicity and for their sufficient effectiveness in resolving natural colors. Within our framework developed here, however, better models of basis functions (such as the first three of Cohen's reflectance basis functions [12] and those of Judd's illuminant basis functions [13]) can be used.

For the three-dimensional linear model, surface reflectance and illumination can be represented as a weighted sum of basis functions expressed as:

$$S(x, y, \lambda) = \sum_{i=0}^{2} \sigma_i(x, y) S_i(\lambda), \tag{1}$$

$$E(x, y, \lambda) = \sum_{j=0}^{2} \varepsilon_j(x, y) E_j(\lambda), \tag{2}$$

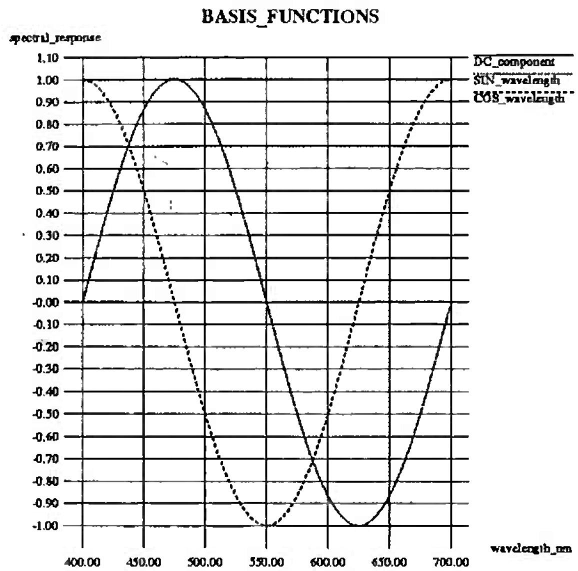


Figure 1: Fourier basis functions

where $S_i(\lambda)$ and $E_j(\lambda)$ are the basis functions, and $\sigma_i(x,y)$ and $\varepsilon_j(x,y)$ are the scalar weighting factors at $(x,y)$. The basis functions

$$S_0(\lambda) = 1,\ S_1(\lambda) = sin\lambda,\ S_2(\lambda) = cos\lambda \tag{3}$$

are shown in Figure 1.

The color image sensing is performed with a CCD camera using filters of different spectral responses. The measured color signal $I(x,y,\lambda)$ is obtained as a product of the spectral power distribution ($SPD$) of illumination $E(x,y,\lambda)$ and the spectral response of the surface reflectance function $S(x,y,\lambda)$, i.e.,

$$I(x,y,\lambda) = E(x,y,\lambda) \cdot S(x,y,\lambda). \tag{4}$$

With 3 filters (usually R, G and B), the quantum catch or the measured signal from the camera is given by

$$\rho_k(x,y) = \int_{\lambda_1}^{\lambda_2} I(x,y,\lambda) \cdot Q_k(\lambda) d\lambda, \tag{5}$$

where $Q_k(\lambda)$ and $\rho_k(x,y)$ for k = 0, 1, 2 are the spectral response of the $k-$th filter and the camera output through the $k-$th filter at $(x,y)$, respectively. The wavelengths $\lambda_1 = 400\ nm$ and $\lambda_2 =$

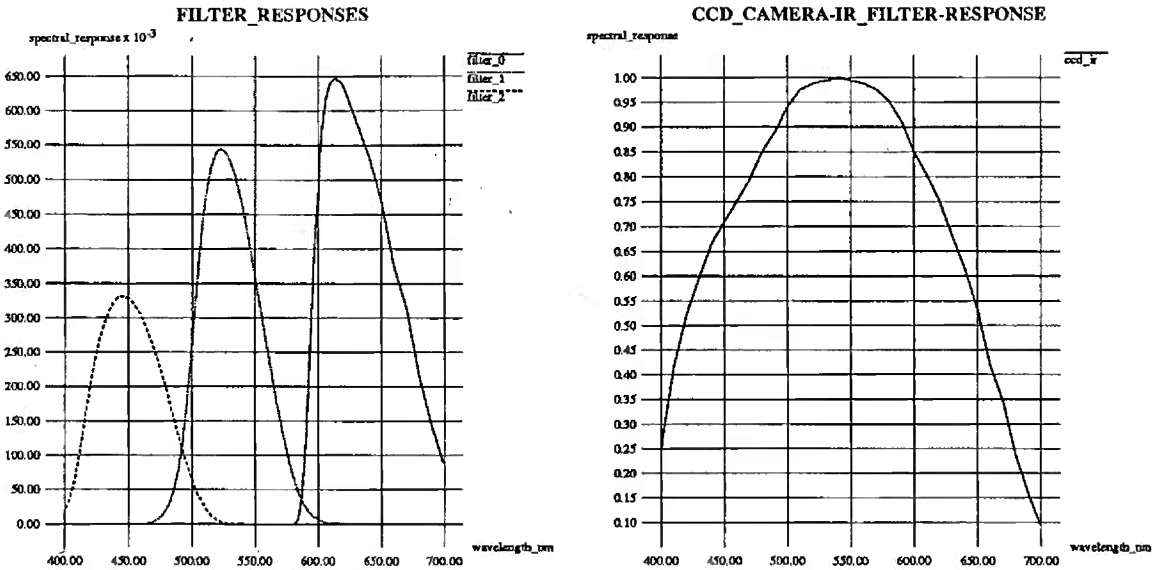


Figure 2: (a)Spectral responses of 3 filters. (b) Spectral response of CCD and IR filter

700 $nm$ cover the range of the visible spectrum. Figure 2 (a) shows the spectral response of the 3 filters: $Q_0(\lambda)$, $Q_1(\lambda)$ and $Q_2(\lambda)$. The curves are obtained from filter measurements with a spectrophotometer and are multiplied by the product of the spectral sensitivity of the CCD camera and the infra-red cut-off ($IR$) filter which is shown in Figure 2 (b). The filters integrate the spectral responses over the given range, and consequently act as an anti-aliasing filter in sampling the color signal.

With 3 basis functions, the relationship between the sensor response, illumination and reflectance is given as

$$\rho = \mathbf{\Omega}^{\sigma}\varepsilon = \mathbf{\Omega}^{\varepsilon}\sigma \tag{6}$$

where the elements of $\Omega^{\sigma}$ and $\Omega^{\varepsilon}$ in the $k$-th row and $j$-th (or $i$-th) column are respectively

$$\Omega^{\sigma}_{kj} = \int_{\lambda_1}^{\lambda_2} \sum_{i=0}^{2} \sigma_i S_i E_j Q_k d\lambda, \tag{7}$$

$$\Omega^{\varepsilon}_{ki} = \int_{\lambda_1}^{\lambda_2} \sum_{j=0}^{2} \varepsilon_j E_j S_i Q_k d\lambda. \tag{8}$$

# 3 Color Constancy

To obtain the surface reflectance of objects, which is the primary information for image analysis, the influence of illumination should be discounted from the measured color in the image. This process is called color constancy. While the general solution for color constancy with unknown illumination demands complex algorithms and some spectral and/or spatial constraints [15] [6], it is simple to remove the known illumination measured with a reference object. One assumption is that the objects of interest are illuminated by light sources of the same *SPD*, and the reference object is applicable. If we use a reference plate with known reflectance $\sigma^{ref}$, the *SPD* of illumination obtained from

$$\varepsilon^{ref} = (\Omega^{\sigma^{ref}})^{-1}\rho \tag{9}$$

represents the spectral composition of the global illumination throughout the image area. With the normalized $\varepsilon^{ref}_{norm}$, the calculation of

$$\sigma = (\Omega^{\varepsilon^{ref}_{norm}})^{-1}\rho \tag{10}$$

leads to the color signal under whitened illumination expressed as:

$$\begin{aligned} I(x,y,\lambda) &= \varepsilon_0(x,y)\cdot[\sigma_0(x,y)S_0(\lambda) \\ &\quad +\sigma_1(x,y)S_1(\lambda)+\sigma_2(x,y)S_2(\lambda)]. \end{aligned} \tag{11}$$

# 4 Surface Reflectance Model

Once the effects of color illumination have been eliminated, the color image $I(x,y,\lambda)$ represents only the surface reflectance properties multiplied by the illumination intensity $\varepsilon_0$.

The analysis of the color image demands proper models for various optical phenomena of surface reflections. We use the dichromatic model for dielectric materials such as plastic, paper and paint [1] [3]. The surface reflectance of dielectric materials has two different optical properties. Highlights are from specular reflection and depend on the refractive indices of the vehicle materials. On

ther other hand, body or diffuse reflection occurs inside the material due to the pigments. The distribution of pigments determines the color of the exiting light by selectively absorbing certain wavelengths.

The magnitude of the image signal is also affected by geometrical factors such as surface orientation, illumination and viewing directions [16]. So far, we have assumed that the geometrical factors are implicitly included either in $E(\lambda)$ or in $S(\lambda)$. More precisely, the geometrical weighting can be regarded as the local variation of illumination density on a surface patch. However, since the geometrical weighting has different mechanisms for specular and body reflections, it would be convenient to include it in the surface reflectance. If we consider the factors as part of the surface reflectance of the dichromatic model, the surface reflectance can be modeled as

$$S(\lambda) = g_S(\mathbf{G})S_S(\lambda) + g_B(\mathbf{G})S_B(\lambda), \tag{12}$$

where $S_S(\lambda)$ and $S_B(\lambda)$ are the specular and the body reflectance, respectively; $g_S$ and $g_B$ are the geometrical factors for the specular and the body reflection, respectively; and $\mathbf{G}$ is the geometrical variable that accounts for the viewer direction and the source direction, where each is relative to the surface normal. Now $S_S(\lambda)$ and $S_B(\lambda)$ represent the real surface reflectance of object, i. e., *albedos*. For most vehicle materials, the refractive index is weakly dependent on $\lambda$. Thus, $S_S(\lambda)$ is almost constant over the visible range of light, while the body color is determined by $S_B(\lambda)$.

Given that the specular reflection is flat over the spectrum, we can rewrite the color image signal as

$$\begin{aligned} I &= (\varepsilon_0 E_0 + \varepsilon_1 E_1 + \varepsilon_2 E_2)\cdot \\ &\quad [(g_S\hat{\sigma}_{0S} + g_B\hat{\sigma}_{0B})S_0 + g_B\hat{\sigma}_{1S}S_1 + g_B\hat{\sigma}_{2B}S_2], \end{aligned} \tag{13}$$

where

$$\sigma_0 = g_S\hat{\sigma}_{0S} + g_B\hat{\sigma}_{0B}, \quad \sigma_1 = g_B\hat{\sigma}_{1B}, \quad \sigma_2 = g_B\hat{\sigma}_{2B}. \tag{14}$$

By using color constancy, we can remove the terms $\varepsilon_1 E_1$ and $\varepsilon_2 E_2$.

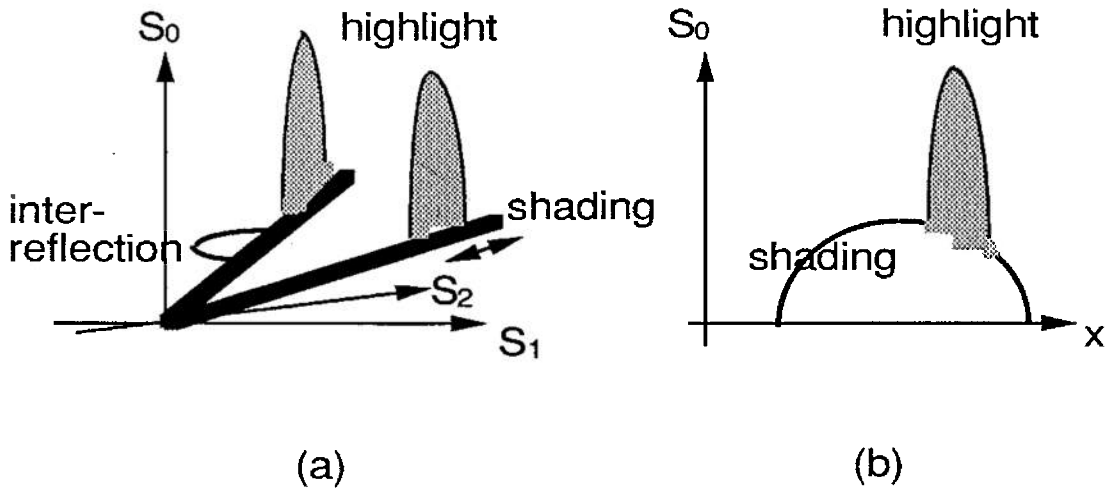


Figure 3: (a)Color clusters on S space, and (b) Spatial variation of intensity due to shading and highlight

## 5 Image Analysis on $(S_0, S_1, S_2)$

For identification of the surface reflection mechanisms explained above, we represent the color on the orthogonal 3-dimensional S space. The S space is similar to the opponent space which is convenient for describing intensity, hue and saturation. The definitions of intensity, saturation and hue for our work are defined as:

$$\begin{aligned} \text{intensity} &= \sigma_0, \\ \text{hue} &= \arctan \frac{\sigma_2}{\sigma_1}, \\ \text{saturation} &= \frac{|\sigma_{12}|}{\sigma_0}, \\ &\quad \text{where } |\sigma_{12}| = \sqrt{(\sigma_1^2 + \sigma_2^2)}. \end{aligned} \tag{15}$$

### 5.1 Shading and Shadow

Shading on surfaces of uniform color is due to variations in geometry G in $g_B(\mathbf{G})$. As can be seen in Equation (13), the shading can be modeled as the weighting of $\sigma\hat{0}_B$, $\sigma\hat{1}_B$ and $\sigma\hat{2}_B$ by the scaling factor $g_B$. This corresponds to a linear cluster of color points through the origin in S space, as shown in Figure 3 (a). Shadows are due to the screening of illumination by other objects, which can be interpreted as the variation of $\varepsilon_0$, $\varepsilon_1$, and $\varepsilon_2$ for a constant factor. Thus the shadow does

not change the shape and the orientation of the linear cluster, but moves the color points toward the origin along the line.

Since the saturation is the slope of this line with respect to the $S_0$-axis, the saturation values of the color points on the linear cluster are constant. The slope of the line can be changed by colored illumination.

## 5.2 Highlight

Since the spectral response of the specular reflection is flat for dielectrics, the illuminating light is reflected from the surface without any change of color. Under white illumination (or whitened illumination by color constancy), highlights add whiteness ($\sigma_{0S}$) to the body colors by $g_S(\mathrm{G})$. As the result, the color points in S space are shifted upward along the $S_0$ direction due to the highlights. In general, the distribution of highlights can spatially vary over the wide area of shaded matte surface as shown in Figure 3 (b), so that they form planar clusters which include the linear clusters made by shading and shadow on the S space as shown in Figure 3 (a). The planes are perpendicular to the $S_1 - S_2$ plane under white illumination or whitened illumination by color constancy.

## 5.3 Inter-reflection

So far we have been concerned only about the first reflection of light. As there are many objects, the object surface of interest receives not only the light from the illumination sources but also the reflected light from the other objects. The latter causes the local change of illumination, as illustrated in Figure 4. The change of surface color due to the multiple reflections between objects is named inter-reflection.

The local influence of the reflected light from other objects is in fact the local variation of illumination. Suppose that we achieve perfect color constancy. In this case the local influence of the

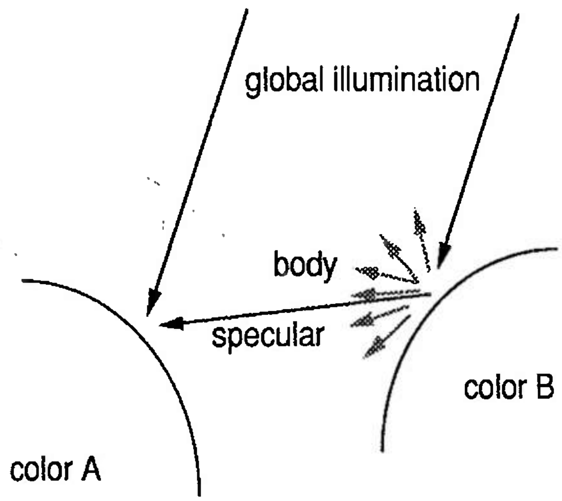


Figure 4: **Inter-reflection**

reflected light from other objects can be discounted together with the global ilumination. However, since we use color constancy for discounting only the global illumination, the inter-reflection remains as a local change of surface reflectance. While large inter-reflection results in a completely different cluster of points, small inter-reflection can be identified as a small deviation from the linear cluster as shown in Figure 3 (a). In general, the color points of inter-reflections do not fall in the planar region formed by highlights and body reflections, since inter-reflection can change the perceived hue as well as saturation of the surface. In Figure 4 the specularly reflected lights from the objects B have the same *SPD*'s as the original illumination since the specular reflectance of dielectrics is spectrally flat. Thus the specular inter-reflections cannot be distingushed from the highlights. On the other hand, the body reflection from the object B produces a local illumination on the object A, inducing a change of the perceived surface color of the object A.

# 6 Image Segmentation

Our segmentation method is based on the assumption that the image consists of patches of object surfaces which have uniform color, i.e., the image can be divided into many regions of uniform hue and saturation regardless of surface structure and finishing.

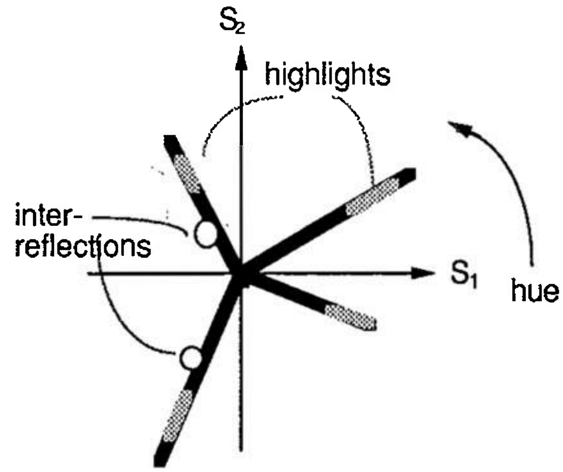


Figure 5: Color clusters in S space (top view)

One of the advantages of having the hue information in addition to the image intensity is that the hue of a surface is more stable than intensity values under changes in the geometrical relationship between the surface normal and the illumination direction. Hue segmentation can be done by hue-histograming or region-splitting based on hue values.

Under white illumination (or whitened illumination by color constancy), the planes formed by highlights and body reflections are perpendicular to the $S_1 - S_2$ plane as shown in Figure 5. Because the highlights are in the same plane as the body color, the specular reflection and the body reflection from the same object are segmented together by the hue segmentation. Without color constancy, the color cluster due to specular reflection is generally not in parallel with the $S_0$ axis, but rather lies parallel to and points in the same direction as the illumination.

Further segmentation and detection of highlights and inter-reflections can be achieved using saturation values. Figure 6 (a) and (b) illustrate the color clusters in the $S_0 - saturation$ plane within a given range of hue values after hue segmentation, and in the projected $S_1/S_0 - S_2/S_0$ plane, respectively. As shown in the figures, since shading and shadow scale $\sigma_0$, $\sigma_1$ and $\sigma_2$ by the same factor, they do not change the saturation value. Thus, an object region with a given color has a constant saturation value. On the other hand, highlights increase only $\sigma_0$ under white

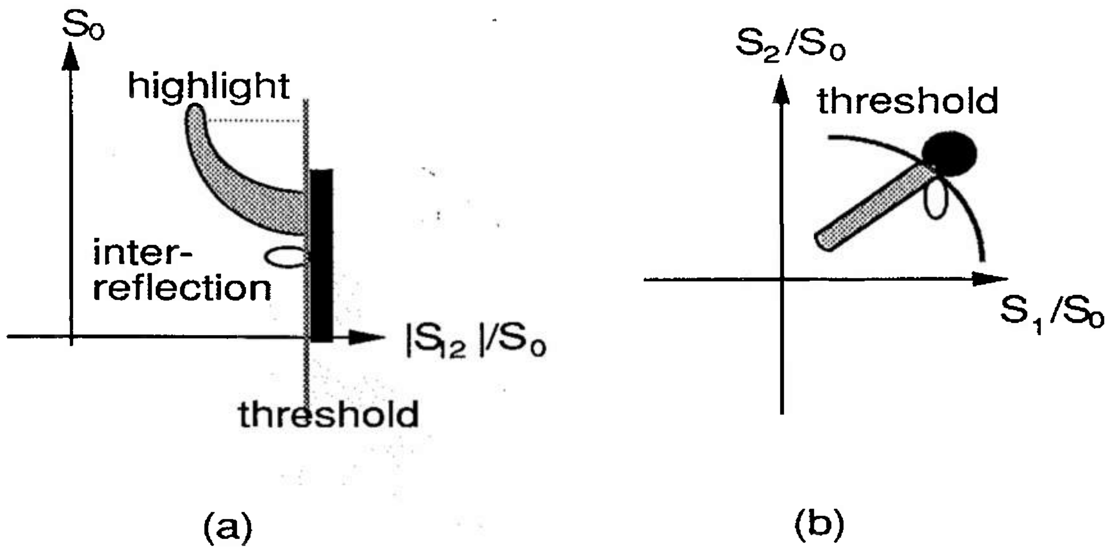


Figure 6: (a) Intensity-saturation plane, and (b) Hue-saturation plane

illumination, thereby always decreasing the saturation. The inter-reflections may affect $\sigma_0$, $\sigma_1$ and $\sigma_2$, which implies that hue and saturation change. Although inter-reflections can possibly increase the saturation or change the hue values of the surface without affecting the saturation value, in most cases they decrease the saturation. This is because the neighboring objects usually decrease the purity of the surface color both by specular and body reflection. Therefore application of local thresholding on saturation values enables us to separate the color clusters of highlights and most of the small inter-reflections from those of body reflections.

## 7 Experimental Results

In order to test the algorithm, we perform an experiment on plastic color balls. Four tungsten lights are used as illumination sources in two directions (right and left sides). They are spatially diffused in order to reduce the contrast between highlights and matte colors. All the measurements are in the linear range of our 8-bit image digitizer, and the camera output is linearized by setting the *gamma* correction factor of the CCD camera to 1. Color constancy is performed using a white reference plate of known spectral reflectance.

Figure 7 (a), (b) shows the intensity ($S_0$) and saturation images and Figure 8 (a) and (b) shows the original image projected on $S_1$, and $S_2$ axes, after the color constancy.

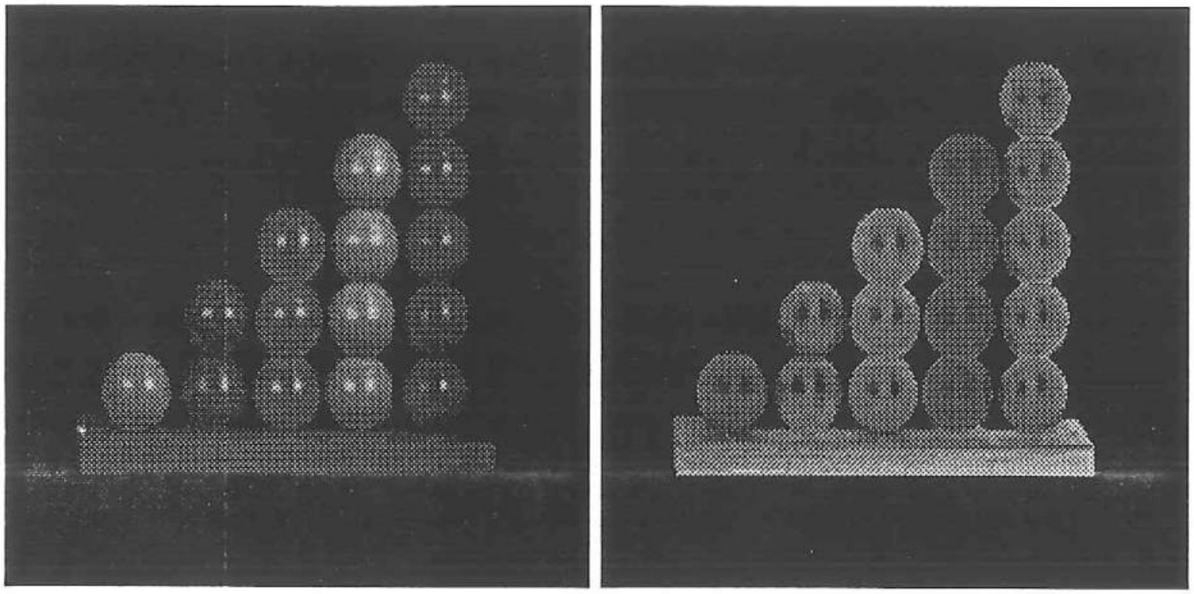

Figure 7: (a) Intensity ($S_0$) (b) Saturation

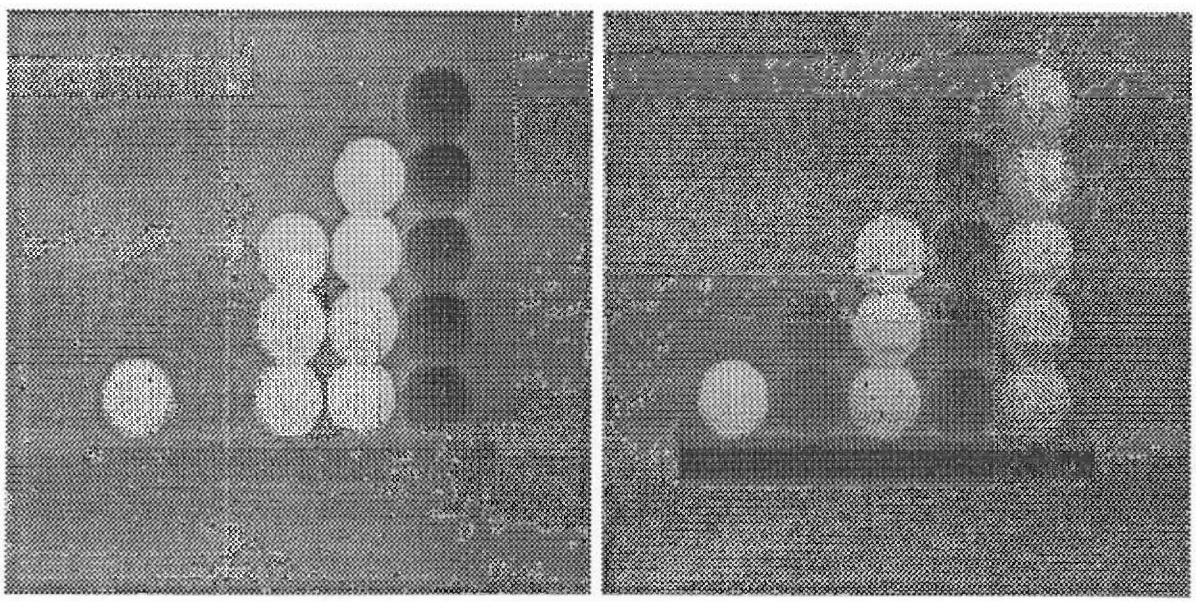

Figure 8: (a) $S_1$ (b) $S_2$

Figures 9 and 10 show the color clusters in S space after implementing color constancy. As expected, the color points from highlights form planar clusters while shading makes linear clusters.

The deviations from the lines and/or planes are due to the errors and noise in measurements as well as the errors in modeling and nonuniformity the surface color.

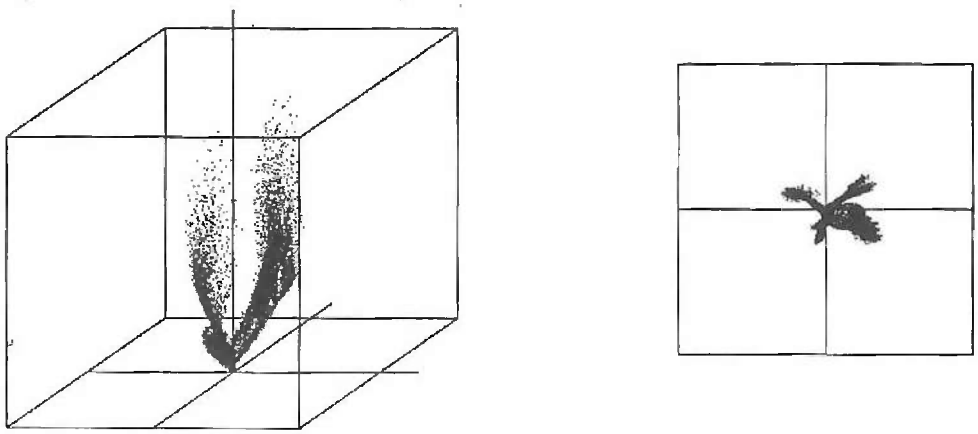

Figure 9: (a) Perspective view (b) Top view

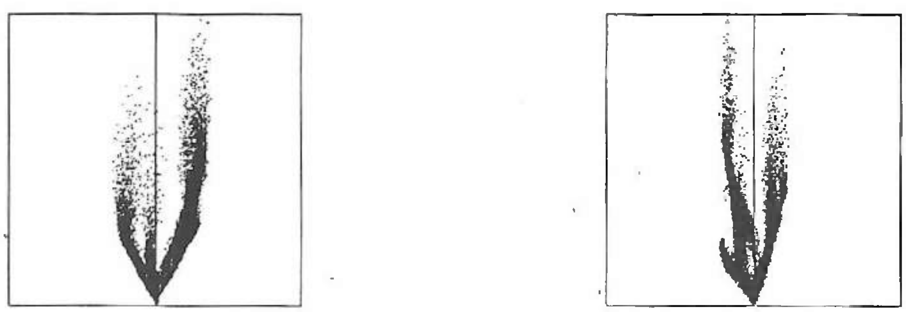

Figure 10: (a) Front view (b) Side view

Hue segmentation is achieved using the hue-histogram shown in Figure 11. The results are partially shown in Figure 12 and Figure 13. After the hue segmentation, application of local

thresholding in each segment results in the separation of body reflections from highlights and inter-reflections. Figure 14 (a) shows separated highlights and inter-reflections which are the deviations from the linear clusters of body reflections. Most of the strong inter-reflections are due to the specular-specular reflections, since the specular reflection is much stronger than the body reflection. The separated body reflections are shown in Figure 14 (b). Inter-reflections are most apparent between objects of different colors.

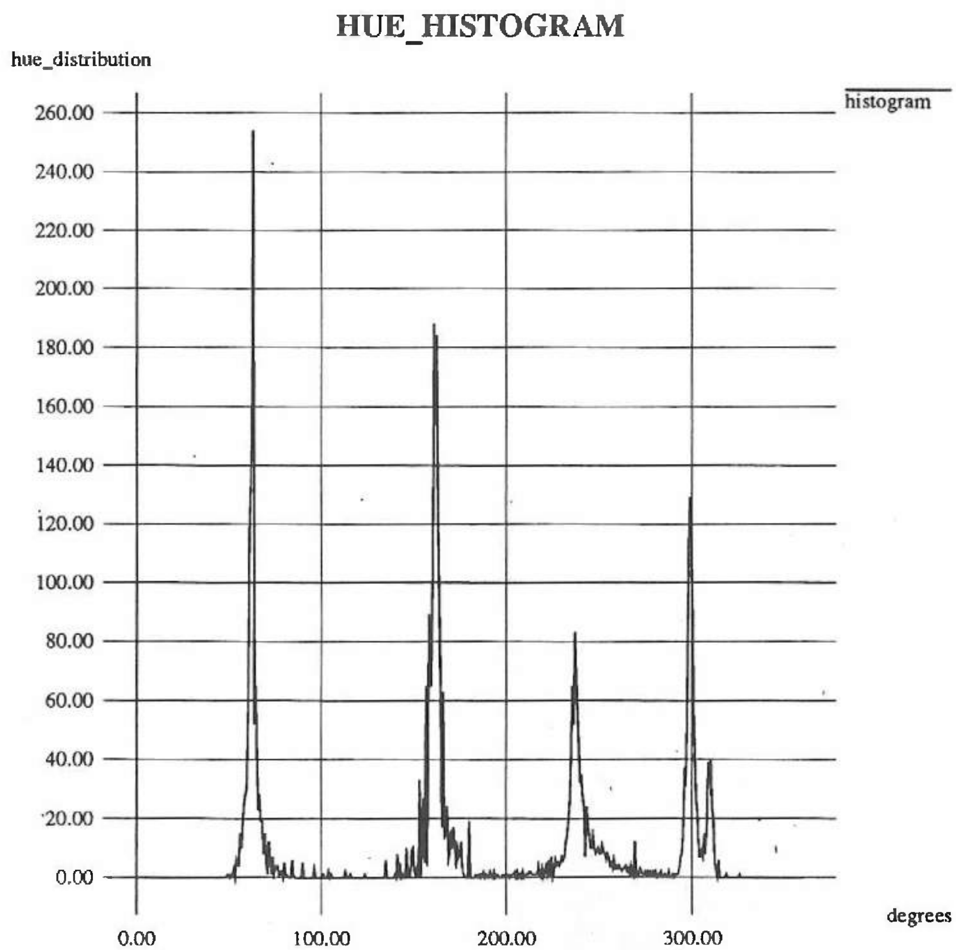


Figure 11: Hue histogram

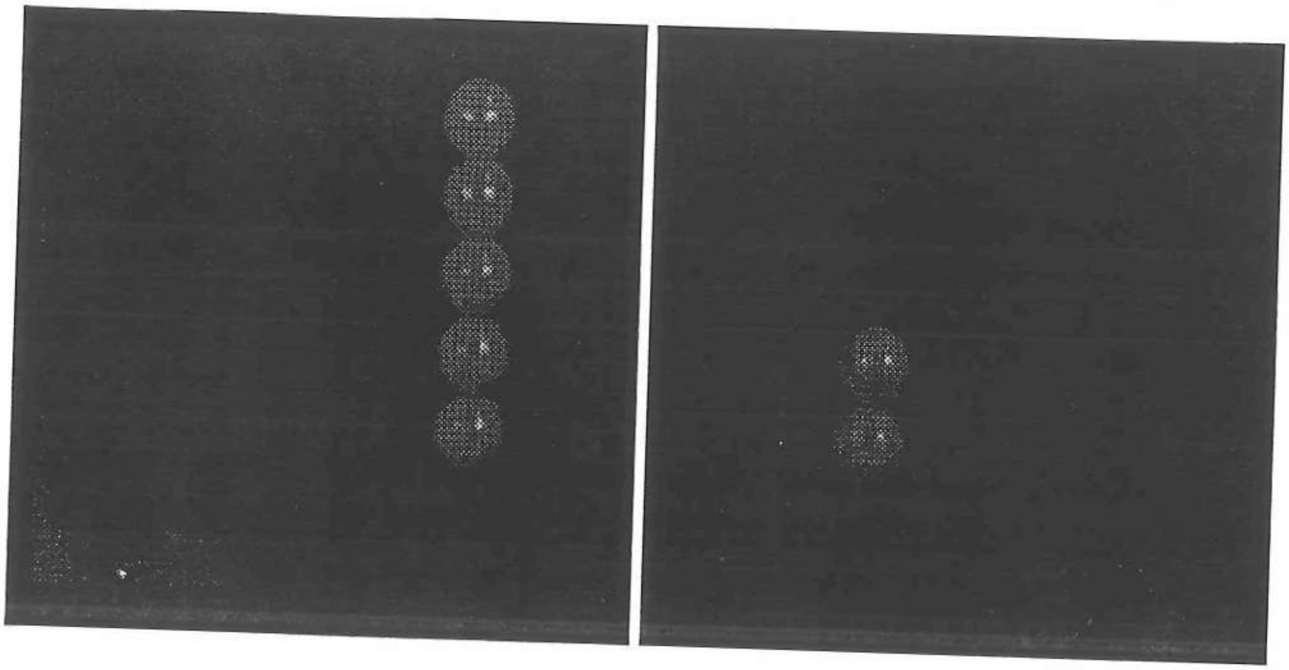

Figure 12: (a) Blue (b) Green

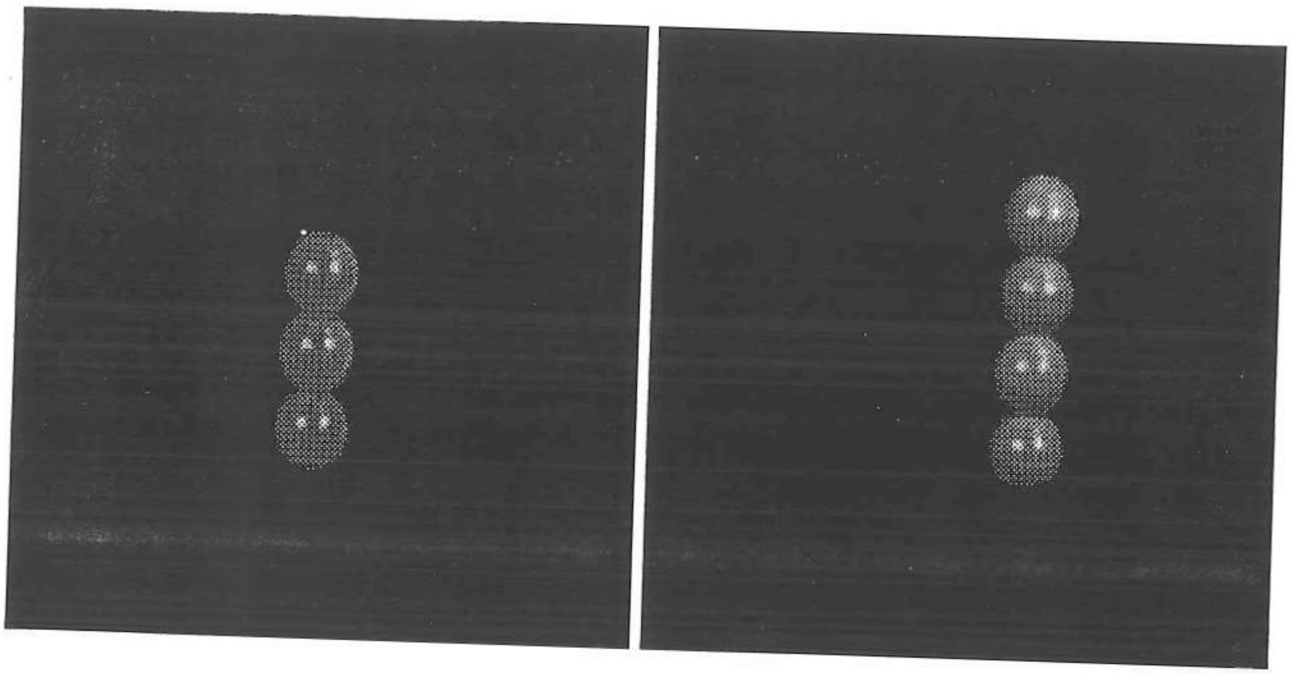

Figure 13: (a) Red (b) Yellow

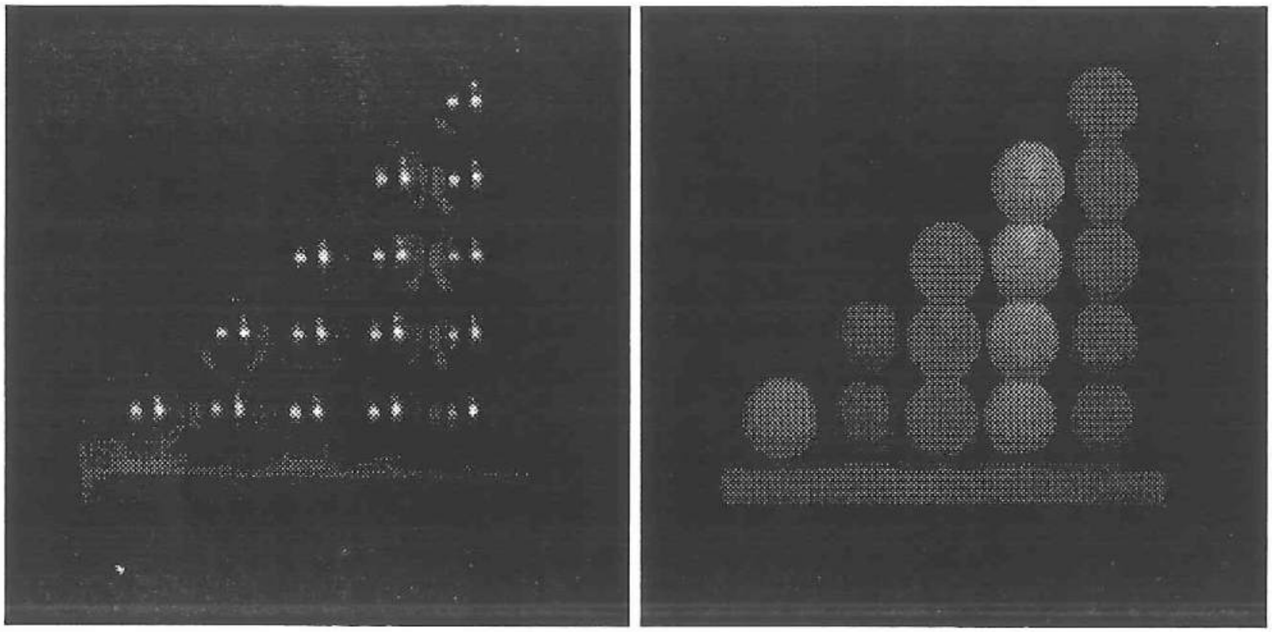

Figure 14: (a) Highlights and inter-reflections (b) Matte

## 8 Discussion

We use objects of saturated colors for our initial experiments in order to demonstrate the efficacy of the algorithm under the assumption that objects consist of surface patches of uniform hue and saturation (not intensity). The segmentation is performed only in S space without using any spatial information. Since separated regions of similar color can be segmented together, segmentation of more complex scenes requires partitioning an image in the spatial domain. Therefore, the use of spatial information is desirable in order to further improve the segmentation.

As mentioned earlier, the deviations of surface colors from linear clusters of shading result from any measurement errors and noise as well as from the non-uniformity of pigment density. Errors can also be generated in the color constancy even with the reference object due to the finite-dimensional representations of surface reflectance and illumination. Another important issue is the proper determination of the local thresholds on the saturation values, since this is the key to the successful detection of highlights and inter-reflections. For our sample image, we obtained the threshold values

by examining the deviation in the saturation values in uniform color regions. We found that the size of the deviations across different parts of the image is about the same. Therefore, the observed deviation values can be used for determining thresholds for any measurements from the same experimental settings. The detection of highlights and inter-reflections can be further improved by locally adaptive adjustment of thresholding. With proper local thresholds, the algorithm is successful in detecting small highlights and inter-reflections which cannot be easily clustered in S space. Note that the separated inter-reflections do not represent the real color of local illumination since the color change due to the inter-reflections is a multiplicative process.

So far we have used a reference object for color constancy. This was based on the assumption that global illumination sources have the same *SPD*. As we have more illumination sources of different *SPD*'s we need general color constancy algorithms to account for spatial variation of illumination. Most of the color constancy algorithms suggested so far require the constraint that illumination varies smoothly in space. When the illumination sources are relatively close to objects and the objects are highly structured, the illumination also varies highly in space depending on the surface orientations. Furthermore inter-reflections do not appear smooth in general. Although small inter-reflections can be detected and removed by observing the change of surface color, large inter-reflections produce completely different clusters of color points which can only be separated by color constancy. Currently we are developing a color constancy algorithm which can resolve highly varied illumination in space.

## 9 Conclusion

In this technical report we present an approach to color image segmentation with the detection and separation of highlights and inter-reflections between objects. To better represent and process the image color, a color metric space is developed based on the physical model of the camera and filters.

The measured color in R, G, B space is transformed into the metric space on a set of orthogonal basis functions. With uncorrelated orthogonal values, we can manipulate each component of color separately or in combination. Since the usual illumination is spectrally colored, calibration of the measured image is performed with a white object of reference to whiten the illumination. While the spectral distribution of the object surface is not changed by shading and shadow under the white illumination, it is affected by highlights and inter-reflections between the objects. As the highlights add whiteness to the object color, they can be detected by observing the change in saturation of the uniformly colored objects. The inter-reflections are also detected with the change in saturation, as well as in hue values. The experimental results show that within the framework, our model of color image interpretation performs well.

## Acknowledgement

This work was supported by the DuPont Corporation and by the following grants: Air Force AFOSR F49620-85-K-0018, ARPA N00014-88-K-0630. We would like to thank F. Fuma and H. Anderson for their help in the experimental setup, and A. Garito, C. Grossman and J.W. Wu in the Department of Physics for their help in the spectral measurements of camera and filters. We would also like to thank S. Shafer and L. Maloney for their helpful suggestions when we were initiating our color work.

## References

[1] S. A. Shafer, "Using Color to Separate Reflection Components", *COLOR Research and Application*, **10**, No. 4, pp 210-218, Winter, 1985.

[2] G. J. Klinker, S. A. Shafer and T. Kanade, "Image Segmentation and Reflection Analysis Through Color", *Proceedings of the DARPA Image Understanding Workshop*, Pittsburgh,

pp. 838-853, 1988.

[3] G. H. Healey and T. O. Binford, "Predicting Material Classes", *Proceedings of the DARPA Image Understanding Workshop*, Pittsburgh, pp. 1140-1146, 1988.

[4] R. Gershon, *The Use of Color in Computational Vision*, PhD dissertation, Department of Computer Science, University of Toronto, 1987.

[5] B. A. Wandell, "The Synthesis and Analysis of Color Images", *IEEE Trans. on PAMI* **9**, No.1, pp. 2-13, January 1987.

[6] L. T. Maloney and B. A. Wandell, "A Computational Model of Color Constancy", *Journal of the Optical Society of America* **1**, No. **1**, pp 29-33, April 1986.

[7] L. T. Maloney, "Evaluation of Linear Models of Surface Reflectance with Small Number of Parameters", *Journal of the Optical Society of America* **3**, No. 10, pp 1673-1683, October 1986.

[8] M. D'Zmura and P. Lennie, "Mechanisms of Color Constancy", *Journal of the Optical Society of America* **3**, No. 10, pp 1662-1672, October, 1986.

[9] R. Nevatia, "A Color Edge Detector and Its Use in Scence Segmentation" *IEEE Trans. on Systems, Man, and Cybernetics* **7**, No. 11, pp 820-826, 1977.

[10] R. Ohlander, K. Price and D. R. Reddy, "Picture Segmentation Using a Recursive Region Splitting Method", *Computer Graphics and Image Processing* **8**, No. 3, December 1979.

[11] O. D. Faugeras, "Digital Color Image Processing Within the Framework of a Human Visual Model", *IEEE Trans. on Acoustics, Speech, and Signal Processing* **27**, No. 4, pp 380-393, August, 1979.

[12] J. Cohen, "Dependency of the Spectral Reflectance Curves of the Munsell Color Chips", *Psychon. Sci.* **1**, pp 369-370, 1964.

[13] D. B. Judd, D. L. MacAdam, and G. W. Wyszecki, "Spectral Distribution of Typical Daylight as a Function of Correlated Color Temperature", *Journal of the Optical Society of America* **54**, p 1031, 1964.

[14] G. Buchsbaum and A. Gottschalk, "Chromacity Coordinates of of Frequency-limited Functions", *Journal of the Optical Society of America* **1**, p 885, 1984.

[15] G. Buchsbaum, "A Spatial Processor Model for Object Colour Perception", *J. Franklin Inst.* **310**, pp 1-26, 1980.

[16] B.K.P. Horn, **Robot Vision**, The MIT Press, 1986.